Physics in Collision - Stanford, California, June 20-22, 2002

LOW x PHYSICS AT HERA

Robin Devenish
Representing the H1 & ZEUS Collaborations.
Oxford University, Physics Department
Denys Wilkinson Bldg, Keble Rd
Oxford OX1 3RH, UK

ABSTRACT

Data on low x physics from ZEUS & H1 are presented and their interpretation discussed. The focus is on the increasing hardness of the energy dependence of inclusive $\gamma^* p$ scattering and certain diffractive processes as the transverse size of the probe decreases.

1 Introduction

HERA remains a unique facility, the only $e^{\pm}p$ collider. With 27.5 GeV $e^{\pm}$ beams on 920 GeVprotons the centre of mass energy is 318 GeV which also gives the upper bound on momentum transfer and thus the scale to which proton structure can be probed. Apart from extending the study of deep inelastic scattering and partonic physics, HERA also allows $\gamma^* p$ interactions to be study over a wide range of photon virtuality down to almost real photons. It provides a unique laboratory in which the high energy behaviour of cross-sections may be studied as a function of the transverse size of the projectile. This is the realm of 'low x' physics. This brief survey covers: the data from H1 and ZEUS on inclusive and diffractive processes: their analysis using perturbative QCD and other models, particularly colour diople models; the evidence or otherwise for universality and gluon saturation at low x.

2 Formalism and phase space

Inclusive electron–proton scattering at HERA $ep \to eX$ is shown in Fig. 1 – LH. At a fixed centre of mass energy, $\sqrt{s}$, where $s = (k+p)^2)$ the process is described by two kinematic variables, Q^2, the four-momentum transfer squared and Bjorken x where

$$Q^2 = -q^2 = -(k-k')^2 : \quad x = Q^2/(2p.q). \tag{1}$$

The inelasticity, $y = (p.q)/(p.k)$, the fractional energy loss of the electron in the proton rest frame, is related to x and Q^2 by $Q^2 = sxy$. The primary measured quantity is the double differential cross-section which, for $Q^2 << M_Z^2$, may be written in terms of two structure functions

$$\frac{d^2\sigma}{dxdQ^2} = \frac{2\pi\alpha^2}{xQ^4}\Big[(1+(1-y)^2)F_2(x,Q^2) - y^2 F_L(x,Q^2)\Big]. \tag{2}$$

The contribution from $y^2 F_L$, the longitudinal structure function, is small and will be ignored in most of what follows. The inclusive scattering process may also be considered in terms of the total cross-section for $\gamma^* p$ scattering. At small x

$$\sigma^{tot}_{\gamma^* p}(W^2,Q^2) = \frac{4\pi^2\alpha}{Q^2}F_2(x,Q^2), \quad \text{and} \quad W^2 \approx Q^2/x, \tag{3}$$

where $W^2 = (p+q)^2$ is the centre of mass energy squared of $\gamma^* p$ system. So the structure function at small x gives $\sigma^{tot}_{\gamma^* p}$ at high CM energies.
The x, Q^2 region in which inclusive measurements have been made is shown in Fig. 1. The strong correlation between x and Q^2 follows from the constraint $Q^2 = sxy$ and

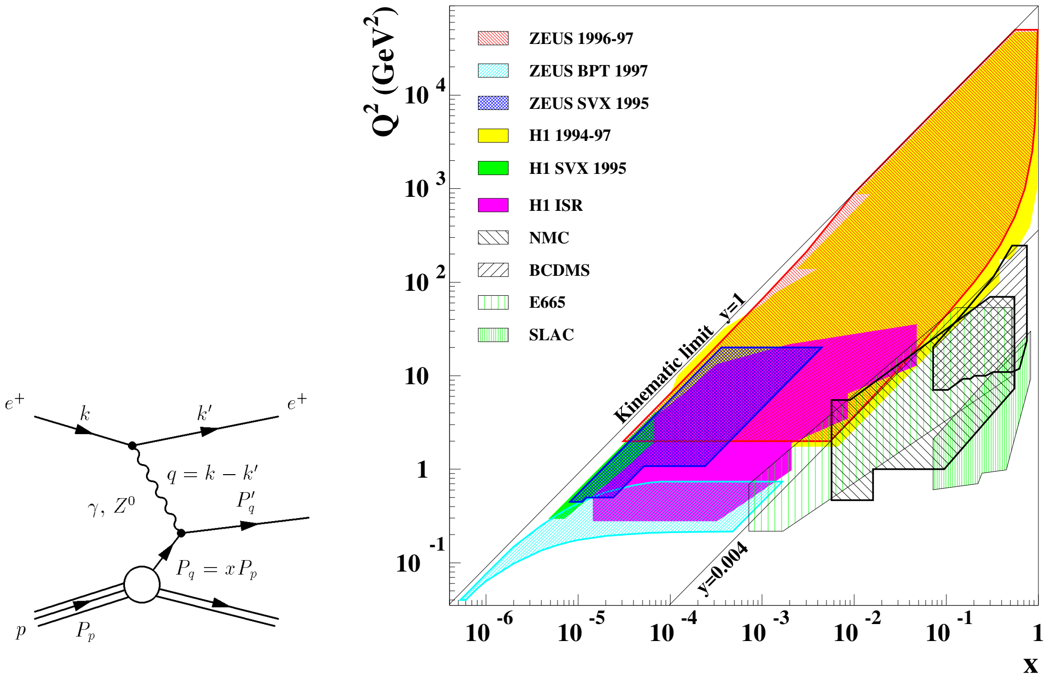

Figure 1: *LH: Inclusive ep scattering and momenta. RH: Kinematic Plane for inclusive ep scattering up to HERA energies.*

the kinematic limit at HERA is given by the line $y = 1$. Fixed target measurements are in the lower right-hand corner of the plot. The region of interest for this talk is roughly $x < 0.01$, and $Q^2 < 250\,\mathrm{GeV}^2$.

3 Contexts

The study of deep inelastic lepton scattering (DIS) and the development of QCD have been intimately related and this continues in the low x region opened up by HERA.[1] The success of pQCD for hard processes relies on factorisation theorems which, in the case of DIS, enables the structure function F_2 to be written in the form

$$F_2(x, Q^2) = \sum_f e_f^2\, x q_f(x, Q^2), \quad \text{with} \quad \frac{\partial q_i(x, Q^2)}{\partial \ln Q^2} \sim \sum_j q_j \otimes P_{ij}, \tag{4}$$

where q_f is the momentum density function for quark of flavour f and charge e_f, P_{ij} are the QCD splitting functions and the sums run over q and $\bar{q}$. At low x F_2 is largely given by the flavour singlet $q\bar{q}$ sea contribution and the evolution of this term is coupled to that of the gluon. The behaviour of both is dominated by the singular

[1] Much more detail and references to original papers may be found in review article of ref. [1].

behaviour of the gluon splitting function $P_{gg} \sim 1/x$, giving rise to an increase in the gluon density, the $q\bar{q}$ sea and hence F_2 at low x.
The DGLAP equations (Eq. 4), which have been calculated to next-to-leading order (NLO) in α_S and partially to next-to-next-to-leading (NNLO), represent a particular, physically motivated, choice of how higher order corrections are summed. The most general behaviour of the splitting functions may be represented by double sum over terms of the form $(\ln Q^2)^n(\ln 1/x)^m$ and there are other possible choices of summation that may be relevant at low x. One of earliest results of pQCD as applied to DIS was derived by taking the leading log terms in both Q^2 and $1/x$, giving

$$F_2(x, Q^2) \sim \exp\sqrt{(12\alpha_s/\pi)\ln(1/x)\ln(Q^2/Q_0^2)}. \tag{5}$$

Another approach, taken by Balitsky et al (BFKL), involves summing the $\ln(1/x)$ terms and gives the striking prediction that $F_2 \sim x^{-\lambda}$, where $\lambda \approx 0.5$ at leading order and fixed α_S. For running α_S and NLO, the corrections to this result are large and are still subject to much. Despite the uncertainty surrounding the exact prediction, the BFKL approach has been of seminal importance in low x QCD dynamics. The DGLAP and BFKL approaches represent two 'extreme' choices in how the tranverse momenta of the radiated gluons are ordered. All calculations agree that gluon dynamics dominates at low x and that the gluon density will increase as x decreases. At some point the gluon density will be so large that non-linear gluon recombination effects will need to be taken into account. A very crude estimate suggests that such effects may occur for Q^2 values for which the gluon-gluon cross-section times the gluon density is of order the proton size:

$$\frac{\alpha_S(Q^2)}{Q^2} xg(x, Q^2) \sim \pi R^2, \tag{6}$$

where R is the proton radius and xg the gluon density. The effect is to slow the rise of F_2.
Hadronic total cross-sections involve soft physics which cannot be calculated perturbatively. Regge theory provides a framework for describing the high energy behaviour of total cross-sections. One expects $\sigma^{tot}_{hadrons} \sim A \cdot W^{2(\alpha_P(0)-1)}$, where A is a process dependent constant and $\alpha_P(0)$, the intercept of the 'Pomeron trajectory'[2], is process independent. Although the value of $\alpha_P(O)$ is not given, the model has been successfully applied to a wide range of hadron-hadron and real photoproduction data, giving a fitted value of roughly 1.093(2) [2]. If these ideas also apply to

[2] In principle α_P is determined by the exchange of states with vacuum quantum numbers in the crossed channel.

$\gamma^* p$ scattering, using Eq. 3, one might expect $F_2 \sim x^{1-\alpha_P(0)}$ at small x. Using the hadronic value of $\alpha_P(0)$ predicts a rather gradual rise $F_2 \sim x^{-0.09}$, with the exponent independent of Q^2. The BFKL calculation may be viewed as an attempt to calculate $\alpha_P(0)$ perturbatively. Quasi-elastic scattering processes, such as diffraction, should also be dominated by the exchange of vacuum quantum numbers and the Pomeron, which is why they are important in unravelling the secrets of low x dynamics.

4 F_2 at low x

Fig. 2 shows F_2 data from H1, ZEUS and the NMC fixed target experiments, plotted as a function of x in bins of Q^2. The right-hand plot, for $Q^2 = 15\,\mathrm{GeV}^2$ well into the deep inelastic range, shows F_2 rising steeply as x decreases. The left-hand plots show bins with Q^2 decreasing from 3.5 to 0.35 GeV^2. Here the rise is still evident at the larger Q^2 values, but diminishes rapidly as Q^2 decreases below $\sim 1\,\mathrm{GeV}^2$. From Eq. 3 the rapid rise of F_2 at small x implies that $\sigma^{tot}_{\gamma^* p}(W^2, Q^2)$ increases more rapidly with W^2 as Q^2 increases, which is not expected in the hadronic Regge framework.

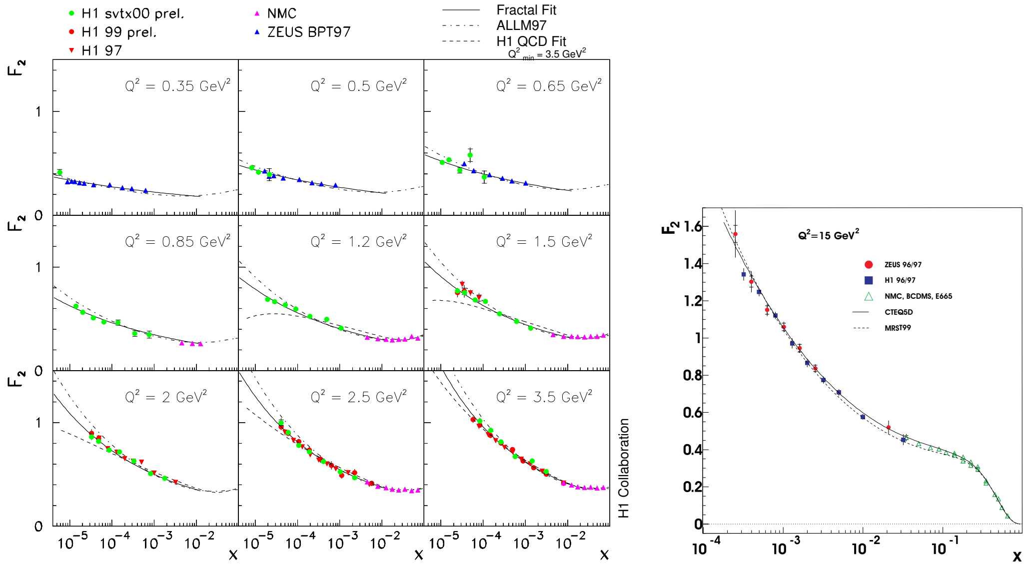

Figure 2: *F_2 data from H1, ZEUS & NMC as a function of x in bins of Q^2.*

H1 have made a model independent study of the rise of F_2 [3]. Using data with $x < 0.01$, the logarithmic slope with respect to $\ln x$ is calculated using

$$\lambda(Q^2) = -\left.\frac{\partial \ln F_2}{\partial \ln x}\right|_{Q^2}, \qquad \text{or} \quad F_2(x, Q^2) = c(Q^2) x^{-\lambda(Q^2)}. \tag{7}$$

The data from HERA are now sufficiently extensive and precise for λ to be measured in bins of Q^2 over a range of x values. At fixed Q^2, λ is found to be independent of x for $x < 0.01$. Fig. 3 shows λ and c as functions of Q^2 where the errors have been calculated using the full systematic and statistical errors of the F_2 data including correlations. At low values of $Q^2 < 1\,\mathrm{GeV}^2$, the value of λ is not far above the value expected from the hadronic Regge parameterisation, whereas at larger values of Q^2, λ rises almost linearly with $\ln Q^2$ to a value around 0.3 at $Q^2 \approx 100\,\mathrm{GeV}^2$. The results for $c(Q^2)$ are roughly independent of Q^2 with a value of about 0.18. The data show no indication that the rate of rise is starting to moderate at larger Q^2, as might be expected from gluon saturation. Similar results for the logarithmic slope have been found in a preliminary analysis of ZEUS data [4].

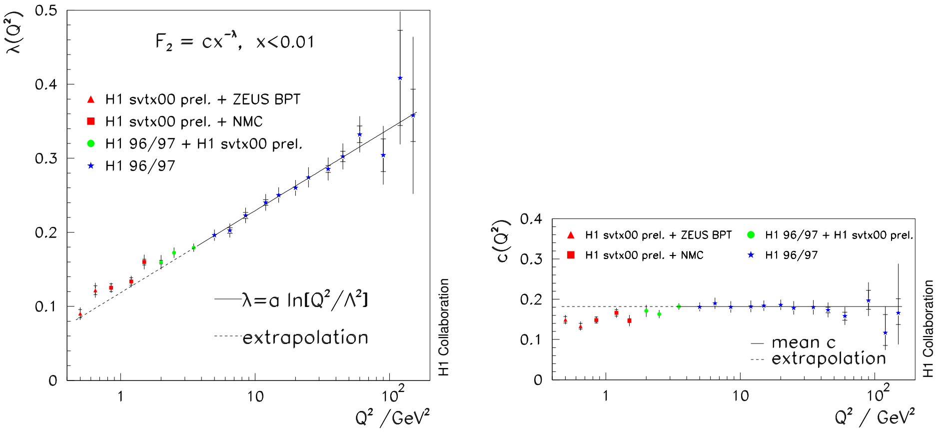

Figure 3: *The logarithmic slope and constant versus Q^2 from the $F_2(x, Q^2) = c(Q^2)x^{-\lambda(Q^2)}$ fit to data with $x < 0.01$. The F_2 data used is mostly from H1 with some very low Q^2 points from ZEUS [3].*

Although the results from the λ analysis support the hypothesis of gluon dominance at low x, it is not possible from this study alone to say which of the pQCD approaches fits best. More information may be gained by applying the models discussed in Sec. 3 to the F_2 data over the full range of HERA and fixed target measurements. The most detailed fits are those using NLO DGLAP to determine the nucleon parton momentum densities. More details are given in the talk by Milstead [5], but the quality of the fits may be judged from Fig. 2 which shows that NLO DGLAP can describe F_2 for Q^2 values larger than $1.5 - 2\,\mathrm{GeV}^2$ and all x values. For other pQCD approaches, fits to the low x F_2 data of comparable quality are obtained but the predictions for other observables, for example F_L, differ quite considerably. Although F_L has been extracted in the HERA kinematic region [6], the data do not yet have the precision to distinguish between the models.

5 Universality at low x?

The F_2 data show gluon and $q\bar{q}$ sea dominance at low x. As the influence of the valence quarks is also small, the possibility arises that this behaviour could, in some sense, be 'universal'. To test this idea the structure function of another hadron must be extracted. Both ZEUS and H1 have published data on the process $ep \to enX$

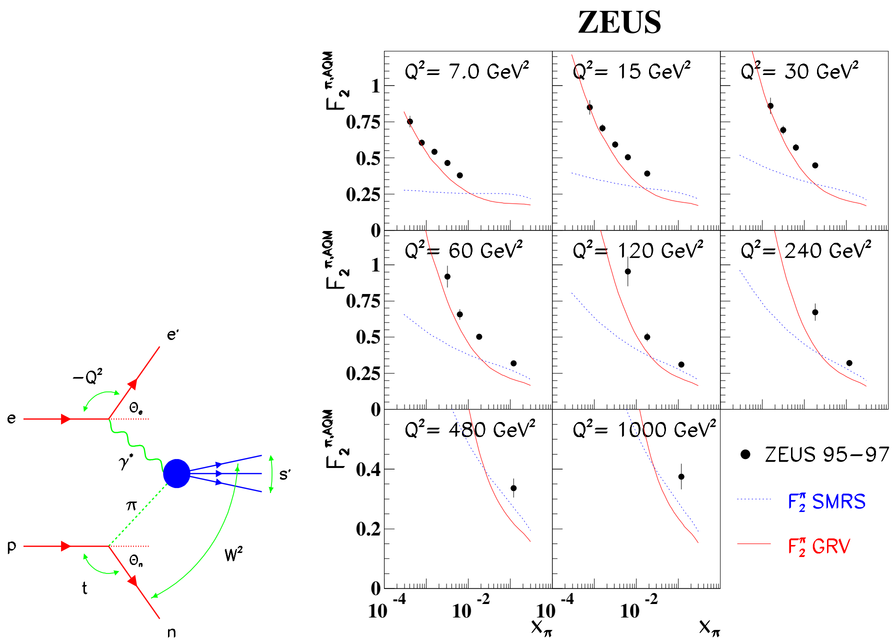

Figure 4: *$ep \to enX$ at HERA: (a) diagram for pion exchange; (b) the pion form factor extracted from the data at small t. From [7].*

([7, 8]). The neutron emerges at a very small angle with respect to the proton beam direction and is measured in a dedicated neutron counter at a distance of the order of 100 m downstream from the main detectors. Knowing the energy and angle of the neutron allows the momentum transfer squared at the $p-n$ vertex, t, to be calculated. At very small values of t, the process is dominated by charged pion exchange as shown in the left-hand diagram of Fig. 4. In this region of phase space the cross-section for $\gamma^* p \to nX$ may be written as a convolution of the flux of pions in the proton $f_{\pi/p}$ with the pion structure function F_2^π. The largest uncertainty in the measurement of F_2^π is the pion flux. Current models differ by up to a factor of two, but this does not affect the x dependence which is shown in the right-hand plots of Fig. 4 - in this case $f_{\pi/p}$ has been estimated using the additive quark model.

The data show very clearly that F_2^π rises strongly for x values below 0.01. Thus at a qualitative level the data support the idea of a universal behaviour at small x.

6 Diffraction

The diffractive process $ep \to epX$ is shown in Fig. 5, together with the additional variables needed to describe it beyond x, Q^2 and W^2 already defined: $x_P \approx 1 - p'_z/p_z$, the fractional longitudinal momentum loss of the proton; M_X the invariant mass of the diffractive final state at the γ^* vertex; $\beta = Q^2/(2q.(p-p'))$ is the equivalent of Bjorken x in the fully inclusive case. This talk will concentrate on the W^2 and Q^2 dependence of two classes of diffractive processes: vector meson production for which $M_X = M_V$; inclusive diffraction with $M_X > 3\,\mathrm{GeV}$. Diffractive events are identified either by direct measurement of the scattered proton using a 'leading proton spectrometer' placed very close to the beam line at a large distance from the primary interaction or by the presence of a large rapidity gap in the main detector between the proton direction and the first energy deposits from the particles making up the M_X system. As already mentioned, diffraction is a quasi-elastic process and in many models the underlying physics is closely related to that of the elastic process. In particular in the Regge approach, the high energy behaviour of the total diffractive cross-sections should be controlled by Pomeron exchange.

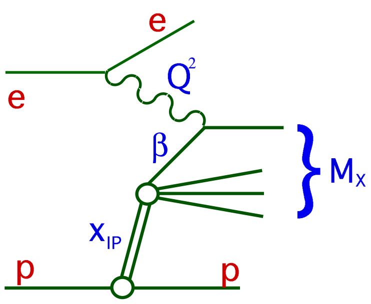

Figure 5: *Diagram and additional kinematic variables for diffraction at HERA.*

6.1 Vector Mesons

First consider the data shown in the LH plot of Fig. 6, $\sigma_{tot}(\gamma p \to Vp)$ for real photoproduction of vector mesons and $\sigma_{tot}(\gamma p \to X)$ and for $W > 10\,\mathrm{GeV}$ the data are fit to a power law dependence $\sigma \sim W^\delta$. For the light vector mesons (ρ^0, ω, ϕ) $\delta \sim 0.22$, not inconsistent with the value expected from Regge theory. For $\gamma p \to J/\psi p$ the energy dependence is much steeper, giving $\delta \sim 0.8$. The RH plot shows δ from the energy dependence of $\gamma^* p \to \rho^0 p$ in fixed Q^2 bins from 0 to $27\,\mathrm{GeV}^2$. Although the errors are large, there is a clear tendency for the energy dependence to steepen as Q^2 increases. In both cases the trend is clear, when there is a hard scale present, either a large M_V or a large Q^2, then the cross-section rises more quickly with energy than expected from soft hadronic physics.

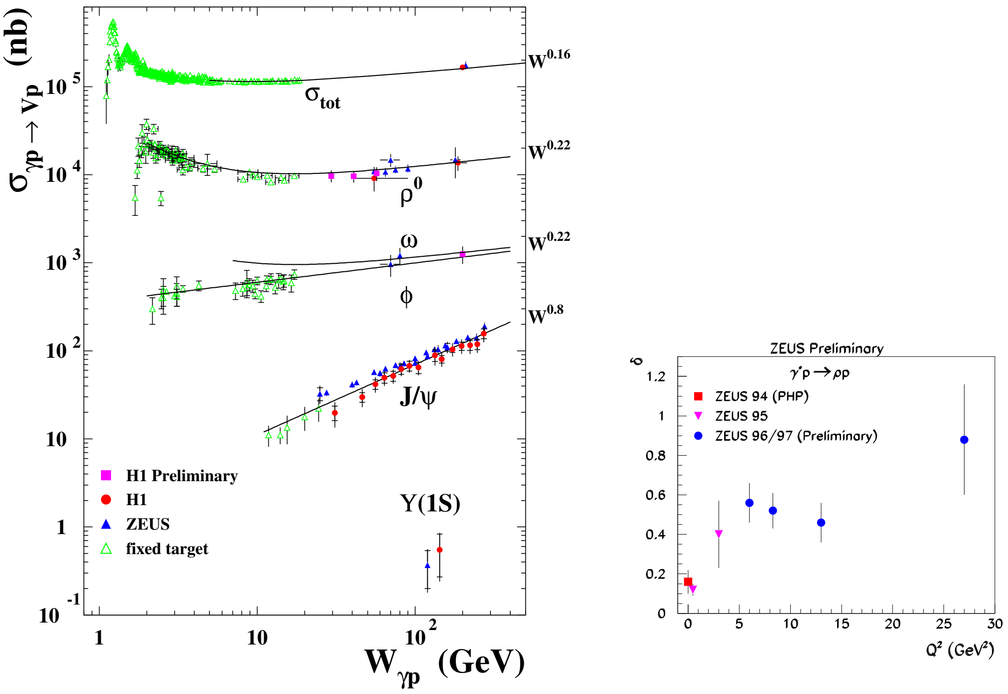

Figure 6: *LH plot, energy dependence of quasi-elastic vector meson photoproduction; RH plot, exponent of the energy dependence of* $\sigma(\gamma^* p \to \rho^0 p)$ *vs* Q^2.

6.2 Inclusive Diffraction

Fig. 7 – LH – shows a ZEUS measurement of the ratio of the diffractive cross-section to the total $\gamma^* p$ cross-section for two values of M_X and 8 values of Q^2 between 0.27 and 60 GeV^2 as a function of W [9]. Assuming Pomeron dominance, Regge theory predicts that the energy dependence of the ration is given by $(W^2)^{2\bar{\alpha}_P - \alpha_P(0) - 1}$ where $\bar{\alpha}_P$ is the value of the Pomeron trajectory evaluated at the mean t of the diffractive data, for the hadronic Pomeron this gives an expectation of $W^{0.19}$. Fitting the ratio data at fixed M_X and Q^2 to a form W^δ gives the results $\delta = 0.24 \pm 0.07$ for data with $Q^2 < 1\,\mathrm{GeV}^2$ and $\delta = 0.00 \pm 0.03$ for data with $Q^2 > 1\,\mathrm{GeV}^2$. Thus, once again, at Q^2 close to photoproduction the data follows the expectation derived from soft hadronic physics, whereas in the deep inelastic region this is not the case and the diffractive cross-section (at fixed M_X and Q^2) follows the energy dependence of $\sigma^{tot}_{\gamma^* p}$.

7 Colour Dipole Models

Many models have been proposed to describe the transition from the soft hadronic-like energy dependence at $Q^2 \approx 0$ to the harder behaviour seen at larger Q^2. In the rest frame of the proton the virtual photon splits into a $q\bar{q}$ pair a long time (or equivalently a large distance) before the interaction. The $q\bar{q}$ pair, characterised by a transverse size r and sharing the longitudinal momentum of the proton in the ratio $(1-z):z$, then interacts with the proton with the cross-section $\sigma_{qq}(x,r)$ giving

$$\sigma^{tot}_{\gamma^* p}(W^2, Q^2) = \int d^2\mathbf{r} dz\, \Psi^*_{\gamma^*}(\mathbf{r}, z, Q^2)\, \sigma_{qq}(x,r)\, \Psi_{\gamma^*}(\mathbf{r}, z, Q^2), \tag{8}$$

where Ψ_{γ^*} is the known wave function for $\gamma^* \to q\bar{q}$. The dipole cross-section has to be modelled and a number of formulations have been proposed [10] and references

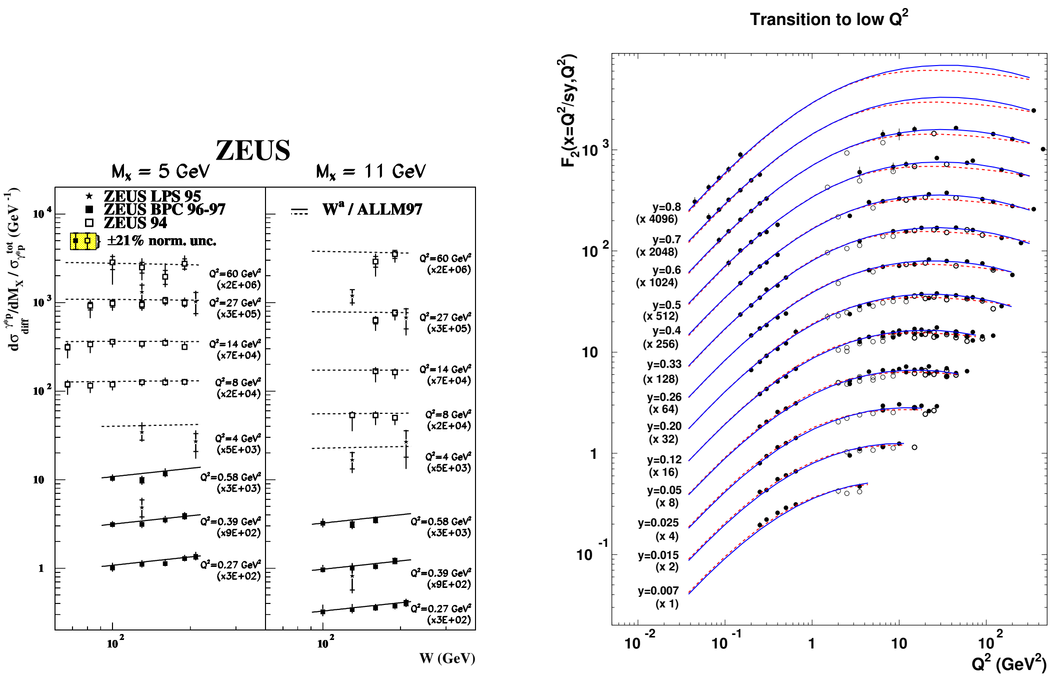

Figure 7: *LH plots: Ratio of inclusive diffraction to $\sigma^{tot}_{\gamma^* p}$ versus W at fixed M_X and Q^2. RH plot: The colour dipole model of Golec-Biernat et al. fit to F_2 data in bins of constant y.*

therein. Here the version of Golec-Biernat & Wüsthoff (GBW) [11] is followed, partly for its simplicity, but also because it builds in the constraint of saturation. In their approach, the dipole cross-section is given by

$$\sigma_{qq}(x,r) = \sigma_0 \left[1 - \exp(-r^2/4R_0^2(x))\right], \quad R_0(x) = (x/x_0)^{\lambda/2}, \tag{9}$$

where σ_0, x_0, λ are three parameters to be determined from data. The interesting features of Eq. 9 are: for small dipole sizes $r << R_0$, $\sigma_{qq} \propto r^2 x^{-\lambda}$; for large dipoles $r >> R_0$, $\sigma_{qq} \propto \sigma_0$ and that the parameter R_0 setting the scale depends on x. This last feature means that the approach to the 'saturation limit' occurs for smaller dipole sizes as x decreases. The parameters of the model are fixed by fitting the HERA low x F_2 data. Another very compelling feature of the dipole approach is that diffraction may also be described. The diffractive cross-section is given by

$$\left.\frac{d\sigma^{Diffr.}_{\gamma^* p}}{dt}\right|_{t=0} = \frac{1}{16\pi}\int d^2\mathbf{r}dz|\Psi(\mathbf{r},z)|^2\sigma^2_{qq}(x,r). \tag{10}$$

Thus no new parameters are required beyond those needed to describe the total $\gamma^* p$ cross-section. The successes of this simple model are a reasonable fit to the low x and low Q^2 (including the transition to the non pQCD region) and the energy independence of the ratio $\sigma^{Diffr.}_{\gamma^* p}/\sigma^{tot}_{\gamma^* p}$ [12]. An obvious deficiency of the model is that it does not contain any mechanism for pQCD Q^2 evolution of the structure function. An attempt to remedy this has been made by Bartels *et al.* [13], the dipole cross-section for small r is modified and related to the gluon density by

$$\sigma_{qq}(r,x) \approx \frac{\pi^2}{3} r^2 \alpha_S \, xg(x,\mu^2), \tag{11}$$

where the scale $\mu^2 \approx C/r^2$ and C is a parameter. The modified model now has 5 parameters to be determined by the F_2 data. The fit to the higher Q^2 data is improved and $\lambda(Q^2)$ (Eq. 7) is well described for all Q^2, whereas for the non-evolving model λ falls below the slope data for $Q^2 > 10\,\mathrm{GeV}^2$. The success of the GBW dipole model cannot be taken to imply that saturation is *required* by the HERA data as other models without saturation, e.g. the dipole model of Forshaw *et al.* [10], fit the data as well.

8 Summary

HERA has provided high precision data on the proton structure function F_2 over a wide range of x and Q^2. In the low x region the bulk of the data is now systematics limit (typical uncertainties are less than 2%). HERA has also provided a wide range of measurements on hard diffractive scattering and quasi-elastic vector meson production. The striking feature of the low x F_2 – the strong rise – is mirrored in diffractive processes when there is a hard scale. The first measurement of the pion structure function at low x shows that it too rises strongly as x decreases, which hints at universality in low x dynamics. The behaviour of low x F_2, or equivalently high energy $\sigma^{tot}_{\gamma^* p}$, is dominated by gluon dynamics. Although some of the important calculations were completed well before HERA started operations, there is no doubt that HERA has opened up new avenues in strong interaction physics.

Particularly the determination of the gluon density at low x, the refinement of high density perturbative gluon dynamics and the deepening of the relationship between diffractive scattering and the physics underlying the rise of total cross-sections with energy. The HERA measurements and the related theoretical developments provide essential input for Run II at the Tevatron, RHIC[3] and the LHC.

9 Acknowledgements

Thanks to my colleagues in ZEUS, H1 and the HERA 'low x club' for providing real and virtual help in the preparation of this talk...

10 References

References

1. A.M. Cooper-Sarkar *et al.*, *Intl. J. Mod. Phys.* A **13**, 3385 (1998).

2. Review of Particle Properties p231, *Eur. Phys. J.* C **15**, 1 (2000).

3. H1 Collaboration, C. Adloff *et al.*, *Phys. Lett.* B **520**, 183 (2001);
J. Gayler, contribution to DIS02, `hep-ex/0206062`.

4. B. Surrow, contribution to EuroHEP 2001, `hep-ph/0201025`.

5. D. Milstead - these proceedings.

6. H1 Collaboration, C. Adloff *et al.*, *Eur. Phys. J.* C **21**, 33 (2001)

7. ZEUS Collaboration, S. Chekanov *et al.*, DESY 02-039, `hep-ex/0205076`.

8. H1 Collaboration, C. Adloff *et al.*, *Eur. Phys. J.* C **6**, 587 (1999)

9. ZEUS Collaboration, S. Chekanov *et al.*, DESY 02-029, `hep-ex/0203039`.

10. J.R. Forshaw *et al.*, *Phys. Rev.* D **60**, 074012 (1999).

11. K. Golec-Biernat & M. Wüsthoff, *Phys. Rev.* D **59**, 014017 (1998).

12. K. Golec-Biernat & M. Wüsthoff, *Phys. Rev.* D **60**, 114023 (1999).

13. K. Golec-Biernat *et al.*, *Phys. Rev.* D **66**, 014001 (2002).

14. P. Steinberg - these proceedings.

[3] See the contribution by Steinberg [14].